



# Groundwater quality and hydrological stress induced by Lower Gondwana open cast coal mine

UJJAL MAL and KALYAN ADHIKARI\*

*Department of Earth and Environmental Studies, National Institute of Technology Durgapur, Durgapur 713 209, India.*

*\*Corresponding author. e-mail: kalyanadhikari99@gmail.com*

MS received 10 March 2020; revised 25 June 2020; accepted 27 July 2020

Open cast coal mine (OCCM) may impose adverse effects on groundwater quality and on its flow regime. Evaluation of water quality often becomes difficult and confusing due to presence of multiple criteria and index based on different parameters. A novel approach has been introduced which speaks about a single index revealing the effect of all important parameters to determine the quality for a particular use of groundwater. Physico-chemical parameters of groundwater are grouped according to their toxicity and the weightage is permitted to each group using analytic hierarchy process (AHP). Overall groundwater quality is found suitable for drinking (DWQI = 1.5–2) and irrigation (IWQI = 2 to 3) purposes in Barjora area. Effect of acid mine drainage (AMD) is not significant in controlling the quality of groundwater in the study area. Carbonate and silicate weathering are the dominant hydro-geochemical processes occurring in the study area. Saturation index derived through Phreeqc Interactive software shows that calcite and aragonite are at supersaturated condition in close proximities of OCCMs. Buffer reactions of carbonate minerals may attenuate the effect of AMD in the study area. The hydrological stress induced by OCCM has been evaluated in OCCM 2 through numerical modelling using MODFLOW software. Evaluation has been performed in three stages of mine development – pre-mining condition, present mining condition and future extension of mine. It is estimated that groundwater of almost 24,163 m<sup>3</sup>/d will ingress into the excavation of 2.03 km<sup>2</sup> area with maximum depth around 200 m from ground level. Model predicted 4–5 m lowering of water table, as an impact, around 2.86 km<sup>2</sup> area of the mine cavity. The irrigation canal passing through this region, will lose 1473 m<sup>3</sup>/d water during future extension of mine.

**Keywords.** Open Cast Coal Mine (OCCM); attenuation of AMD; saturation index; WQI; groundwater flow modelling; drain boundary.

## 1. Introduction

Gondwana coals are the prime source of energy in many countries. In India, Lower Gondwana provides the bulk requirement of coal to the industries. OCCMs are operating in various coalfields (Jharia, Raniganj, Bokaro, Singarauli), where Lower Gondwana coal occurs at shallow depth. These

coalfields are composed of similar lithologic successions (Bhowmick and Ghosh 2002; Vijaya *et al.* 2012; Pal *et al.* 2015). In Australia, equivalent of Lower Gondwana formations of India are observed (Mishra 1996). It is assumed that effect of OCCMs on local hydrogeological environment will be more or less similar in Lower Gondwana coalfields. The mining industries with inappropriate

management carry a number of environmental issues and groundwater pollution is one of them. Apart from groundwater quality, effect of OCCMs on groundwater flow regime is obvious because of development of almost permanent cone of depression associated with continuous pumping from the pit, which in most cases actually reduces the storage of the aquifers linked with the pit. Mining operation itself acquires trouble through seepage of groundwater into the excavation sites. Intrusion of water often leads to operational, economical and safety problems which include flooding, increased drilling costs, delays, slope instability, equipment corrosion, and oxidation of sulphides (Peksezer-Sayit *et al.* 2014). In OCCMs, water bearing layers are exposed along the periphery of mine cavity and act as seepage face. When excavation continues below water table, ponding of water within the depression from surrounding aquifers takes place. Preventing measures like dewatering wells, impervious curtains and drainage pipelines are generally used to avoid groundwater intrusion into the mine (Jiang *et al.* 2013). Dewatering of mine resembles pumping well and as a result of which desaturation of aquifers may take place. Thus, a hydrogeological study is essential prior to the development of mine.

Acid mine drainage (AMD) is a common phenomenon which impacts groundwater quality. Many researchers around the world found dubious distinctions in groundwater quality around the OCCMs. Water quality issues like low pH, high TDS, sulphate and heavy metal concentrations are commonly associated with OCCMs which deteriorate the suitability of water for different uses (Singh *et al.* 2011; Adhikari *et al.* 2013). Bureau of Indian Standards (BIS) and World Health Organization (WHO) have drinking water quality standards based on individual physico-chemical parameters. There is no such standard which assess water quality using overall physico-chemical parameters. Evaluation of water quality often becomes difficult and confusive due to presence of multiple criteria and index based on different parameters. A novel approach has been introduced which speaks about a single index revealing the effect of all important parameters to determine the quality for a particular use of groundwater. From a management point of view, optimization of water quality in association of allied parameters is often more essential than aiming on individual one. Now-a-days, researchers have a tendency to assess overall drinking water standard using water quality index (WQI) (Sahu

and Shikdar 2008; Sadat-Noori 2014; Kumar *et al.* 2015; Shabbir and Ahmad 2015). WQI is a very useful and simplified method, which reduces several parameters into a single number. It is widely used in judging the suitability of groundwater and surface water bodies (Singh *et al.* 2008; Trivedi *et al.* 2009; Rajankar *et al.* 2010; Gebrehiwot *et al.* 2011; Ravikumar *et al.* 2013; Rabeiy 2017). These water bodies are also used in irrigation purpose. Sodium Adsorption Ratio (SAR), Magnesium Adsorption Ratio (MAR), Residual Sodium Carbonate (RSC), Kelly's Ratio (KR) are very useful indices which check the suitability of groundwater for irrigation purpose. Simsek and Gunduz (2007), Adhikari *et al.* (2012), and Narany *et al.* (2016) used WQI to evaluate water quality for irrigation purpose.

In nature, the groundwater quality depends on atmospheric precipitations and recharge conditions. Apart from those various hydrogeochemical processes like rock-water interaction, weathering and dissolution, ion exchange reactions and other chemical reactions can affect the concentration of various ions. Effect of AMD is common on groundwater, but cannot occur everywhere around the OCCMs. Local hydrogeological condition can play key role in attenuation of AMD. Leachate percolation through soil depends upon various environmental factors like hydrological, mineralogical and chemical properties of the soil which in turn affect the heavy metal sorption into the soil. Sorption primarily depends upon type of clay minerals, pH of the solution, dissolved organic matter content, cation exchange capacity, specific surface area, carbonate content and iron oxides content (Low *et al.* 2000). The influence of AMD on the properties of sorption in soil decreases the ability of binding heavy metals to soil particles. But the presence of carbonates at high pH (>7) leads to increase the heavy metal retention capacity of the soil. As the pH decreases, the carbonates get dissolved and ion exchange becomes the principle retention mechanism of heavy metals in the soil (Plassard *et al.* 2000). Mining operation can disrupt the water budget of the region. The proper assessment of groundwater inflow into the mine is also essential for mining authorities to achieve the safe mining goal. The estimation of groundwater seepage is an intricate job. Simple analytical model as well as complex numerical model has been used to evaluate groundwater seepage into the mines by various researchers (Marinelli and Niccoli 2000; Singh and

Atkins 1985; Bochenska *et al.* 2000; Ardejani *et al.* 2003; Fontaine *et al.* 2003; Rapantova *et al.* 2007; Aryafar *et al.* 2009; Brouyere *et al.* 2009; Zaidel *et al.* 2010). Simple analytical models have their limitation in application on field scale. On the other hand, numerical model has ability to predict groundwater seepage rates in complex hydrodynamic conditions more accurately. Surinaidu *et al.* (2014) estimated the groundwater inflows into the coal mines at different mine development stages using MODFLOW in Andhra Pradesh, India. Dhakate *et al.* (2019) assess impact of mining on the Kelo River using MODFLOW in Chhattisgarh, India.

The present study was performed in the OCCM of Lower Gondwana Barjora coalfield. Previously, Adhikari and Mal (2019) assessed the possible source of present groundwater composition in this region. However, effect of OCCMs on groundwater flow regime and its effect on groundwater suitability for different uses have not been assessed. In spite of significant presence of pyrite, the source of AMD generation, i.e., the overburden dump of the study area, the physico-chemical characteristics of groundwater of the region has not witnessed the impact of AMD (Adhikari and Mal 2019). The reason behind it has not been identified. In present scope of study, the authors have tried to assess: (1) impact of OCCMs on groundwater suitability for drinking and irrigation purposes, (2) hydro-geochemical process that retard the effect of AMD in groundwater, (3) temporal change in seepage into the excavation with advancement of mine, and (4) potential impact of dewatering on local groundwater and overall hydrologic system. WQI is used to check the suitability of groundwater for drinking and irrigation purposes. Authors categorised all physico-chemical parameters into groups and tried to improve the weighing excellence among the groups using AHP (Saaty 1980). Hydro-geochemical studies along with GIS mapping technique have been used to understand the natural attenuation of AMD in the study area. The groundwater flow is simulated using MODFLOW 3D finite difference based numerical model and the seepage is predicted using drain package of MODFLOW (Anderson and Woessner 1992). The prediction of this study will help the local authorities to prepare a better policy in groundwater resource management. Further, this study can be used as a reference in other Lower Gondwana coal fields around the world where similar lithologic association and hydrologic setting exist.

## 2. Study area

### 2.1 Geography and climate

The study has been conducted over an area of  $\sim 100 \text{ km}^2$  with latitude of  $23^\circ 29' 39''$ – $23^\circ 23' 18''$ N and longitude of  $87^\circ 12' 29''$ – $87^\circ 21' 04''$ E. The tropic of cancer passes through this region. Generally, it is hot throughout the year and it reaches up to  $\sim 42^\circ\text{C}$  in summer season, while in winter season, it comes down to as below as  $\sim 7^\circ\text{C}$ . Precipitation mainly occurs in rainy season through southwest monsoon during mid-June to mid-September. Almost 85% of total annual rainfall occurs during this time. The average annual rainfall is 1204.5 mm. Topographically, it has gentle southeasterly slope with an average height of 72 m from mean sea level (msl). The watershed of the region is dictated by Damodar River, which is flowing towards east (figure 1). An irrigation canal originating from the southern bank of Damodar River at Durgapur Barrage is flowing towards south and then towards east. The OCCM 1 is present in the western part of the study area at an elevation of 74 m from msl. The OCCM 2 is present  $\sim 5 \text{ km}$  apart from OCCM 1. The OCCM 2 is surrounded by the Damodar River and irrigation canal. OCCM 2 is situated at an elevation of 68 m from msl. Presently, the two OCCMs are at inoperative condition due to legal dispute. The area basically constitutes a part of flood plain of Damodar River and covered with an apron of alluvial sediments. It has been observed that settlements are located in relatively higher contour levels and agricultural land in lower contour levels.

### 2.2 Geology and hydrogeology

Hydrogeological setting along with climate and topography primarily controls the occurrence and movement of groundwater. The study area is underlain by Gondwana Formation. Archean and Gondwana rocks mainly constitute the subsurface lithology, while the alluvial sediments form the thin veneer along the river channels in the topographic depressions. The geological sequence of the study area, reported by Geological Survey of India (GSI) (Das *et al.* 1992) is shown in table 1. A regional exploration done by GSI revealed the presence of five coal seams (Seam-I to Seam-V) within Raniganj Formation and three coal seams within Barakar Formation (Seam-A to Seam-C).

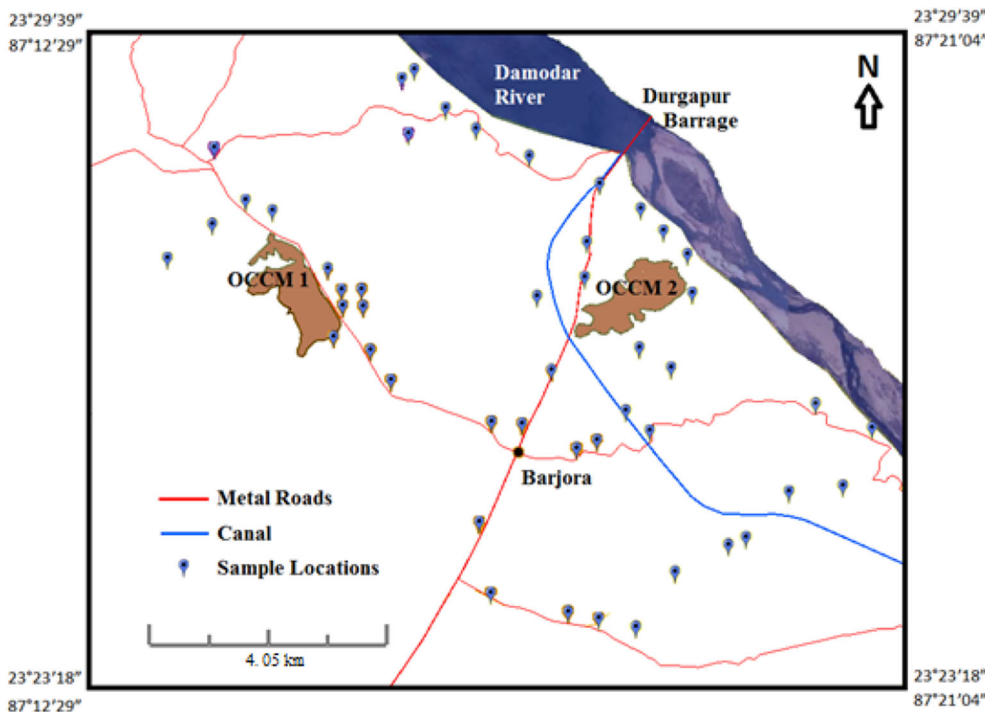


Figure 1. Study area.

Table 1. Lithological succession of the study area (after Das et al. 1992).

Formation	Lithology	Maximum thickness in m
Alluvium	Yellow to buff, micaceous unconsolidated sand and sandy soil, ferruginous soil	46.70
Tertiary deposit	Light grey to silver grey mottled clay, mudstone, siltstone, soft fine grained clayey sandstone, loose sand with sub-angular to sub-rounded pebbles	45.50
Unconformity		
Panchet formation	Pale green- massive-micaceous argillaceous sandstone with reworked shales; green shale cross-bedded at places pebbles toward base	257.50
Raniganj formation	Dirty white fine to medium grained sandstone, coarser at places; grey sandy shale, siltstone, carbonaceous shale and thin coal seams, coarse to very coarse with a few pebbles at base	239.31
Barren measure formation	Dark grey to black shale with arenaceous bands at places	101.49
Barakar formation	Light grey to greyish white-medium to coarse grained feldspathic sandstone, fined grained at places, coarse to pebbly at base, thin coal bands	56.42
Unconformity		
Metamorphics	Quartz granulite, hybrid rock	
Basement complex		

The outcome of the exploration has proved that the most important Raniganj Seam of the area is Seam-II, which occurs at comparatively shallow level. The thickness of the seam varies from 6.17 to 13.25 m (Roy and Ghosh 2002). Two coal seams namely Seam-II and Seam-I are available in the study area for surface mining. Coal Seam-II is found at shallow depth and has an average thickness of

8.25–11.5 m. Whereas coal Seam I is found at relatively greater depth with a thickness of 2.5–4.1 m. The depth of the coal seams has increased towards north and east directions in the study area. The northwest–southeast striking fault plane (normal fault), present in this region, causes deeper placement of the coal seams in north-east direction from the present excavation site.

The Gondwana sediments form the semi-consolidated formations possess better water potential zone. Sandstones and shales are the major lithounits of the Gondwana Formations. Gondwana sandstones, in general, are known to constitute good aquifers at many places. Gondwana basin is typically a rift basin which constitutes a number of faults. These fault plains may act as secondary aquifer. Alluvial sediments constituted unconfined aquifer and in few places, it occurs as semi-confined condition. The regional groundwater flow is towards north to north-east direction (Adhikari and Mal 2019).

### 3. Methodology

#### 3.1 Laboratory and field study

Total 94 groundwater samples (46 post-monsoons and 48 pre-monsoons) were collected from open wells and bore wells of the villages in and around the open cast coal mines of Barjora block. Concentration of sampling was more in the proximity of mine sites in comparison to the areas progressively distant from the mine sites. The samples were collected mainly from the open wells and the water table depths were measured by measuring steel tape. In some locations, samples were collected from tube wells due to absence of open wells. The samples of every location were collected in clean polyethylene bottles of both 1 l and 120 ml capacities. Samples were taken in bottles of 1 l to analyse the anions and for analysis of cations and heavy metal samples were taken in 120 ml bottles. The samples of 120 ml bottles were preserved in pH < 2 condition in field by adding HCl. Before sampling, the bottles were soaked with dilute HNO<sub>3</sub> for a day and were cleaned with deionised water at least three times. They were again rinsed at least twice with the sample water during the time of sampling. Twenty physico-chemical parameters of the groundwater samples were measured. The pH was measured by Eutech pH 510 meter, total dissolved solids (TDS) was measured in Eutech Con 510 meter. Calcium, magnesium, sodium, potassium, iron, arsenic, cadmium, chromium, copper, manganese, nickel, lead and zinc were analyzed using atomic absorption spectrophotometer (AAS) (Perkin Elmer). Fluoride (F) was determined in Orion 4 star pH/ISE meter. Bicarbonate was estimated using titrimetric method, chloride was analyzed in volumetric method by AgNO<sub>3</sub>

titration, nitrate and sulphate were measured by spectrophotometric method in UV-Visible spectrophotometer (Shimadzu, UV1800) (APHA 1995). The standards were prepared to run in AAS from the 1000 mg/l stock solutions (procured from Perkin Elmer). The exactness of the analyses was controlled through running of standards and blanks at frequent interval with calibration curve of  $R^2$  value 0.99. Overall the accuracy of the results was checked through cation-anion balance with error between  $\pm 5\%$ .

#### 3.2 WQI analysis

WQI is a comprehensive and easy tool for decision makers, which transform parametric concentrations into a quantitative index. An innovative WQI technique has been applied in the present study. All physico-chemical parameters were categorized into five groups for both drinking water quality index (DWQI) and irrigation water quality index (IWQI) as the first step in WQI analysis (table 2). Parameters of similar nature and impact on quality of water were grouped together. For DWQI, five groups were identified as (a) toxic metals, (b) toxic anions, (c) TDS & pH, (d) major cations, and (e) miscellaneous. Whereas for IWQI, the five groups were namely (a) salinity hazard, (b) permeability hazard, (c) specific ion toxicity, (d) trace element toxicity, and (e) miscellaneous effect. After categorization of physico-chemical parameters, the relative weightage of each group were assigned using AHP, where pairwise comparisons among the groups were made. The comparisons among the groups were represented by integer value from 1 to 9. Integer value 1 means two criteria (group) are of equal importance and higher number represent greater importance of the criteria to another. Thus a pairwise comparison matrix was formed (table 3). Then a normalized matrix was designed and the eigenvector (weightage) was calculated. The consistency of the comparisons was checked by the equation

$$\text{Consistency ratio} = \frac{CI}{RI}, \quad (1)$$

where  $CI$  is consistency index and  $RI$  is random index. The consistency ratio value should be <0.1 for any set of comparisons (Saaty 1980). In this indexing technique quality rating was also assigned for each parameter of all weighted criteria according to their suitability in the context of



Table 2. Classification of DWQI and IWQI parameters.

Drinking water quality index (DWQI)		Water quality index (WQI)		Irrigation water quality index (IWQI)						
Category	Weightage	Range			Parameter	Weightage	Hazard	Range		
		Suitable (rating = 2)	Unsuitable (rating = 1)					Highly suitable (rating = 3)	Moderately suitable (rating = 2)	Unsuitable (rating = 1)
Toxic Metals	0.35	As ≤ 0.01	As > 0.01	Salinity	0.43		TDS < 450	450 ≤ TDS ≤ 2000	TDS > 2000	
		Cd ≤ 0.003	Cd > 0.003	Permeability	0.32		SAR < 6	6 ≤ SAR ≤ 9	SAR > 9	
		Cr ≤ 0.05	Cr > 0.05				Na% < 40	40 ≤ Na% ≤ 60	Na% > 60	
		Cu ≤ 0.05	Cu > 0.05	Specific ion	0.14		Cl < 140	140 ≤ Cl ≤ 350	Cl > 350	
		Fe ≤ 0.3	Fe > 0.3	Trace element	0.07		As < 0.1	0.1 ≤ As ≤ 2.0	As > 2.0	
		Mn ≤ 0.1	Mn > 0.1				Cd < 0.01	0.01 ≤ Cd ≤ 0.05	Cd > 0.05	
		Ni ≤ 0.02	Ni > 0.02				Cr < 0.1	0.1 ≤ Cr ≤ 1.0	Cr > 1.0	
		Pb ≤ 0.01	Pb > 0.01				Cu < 0.2	0.2 ≤ Cu ≤ 5.0	Cu > 5.0	
		Zn ≤ 5	Zn > 5				F < 1.0	1.0 ≤ F ≤ 15.0	F > 15.0	
		F ≤ 1.5	F > 1.5				Fe < 5.0	5.0 ≤ Fe ≤ 20.0	Fe > 20.0	
Toxic Anions	0.27	NO <sub>3</sub> ≤ 45	NO <sub>3</sub> > 45				Pb < 5.0	5.0 ≤ Pb ≤ 10.0	Pb > 10.0	
		SO <sub>4</sub> ≤ 200	SO <sub>4</sub> > 200				Mn < 0.2	0.2 ≤ Mn ≤ 10.0	Mn > 10.0	
		Cl ≤ 250	Cl > 250				Ni < 0.2	0.2 ≤ Ni ≤ 2.0	Ni > 2.0	
TDS & pH	0.22	TDS ≤ 500	TDS > 500				Zn < 2.0	2.0 ≤ Zn ≤ 10.0	Zn > 10.0	
		pH ≤ 8.5	pH > 8.5	Miscellaneous effect	0.04		HCO <sub>3</sub> < 90	90 ≤ HCO <sub>3</sub> ≤ 500	HCO <sub>3</sub> > 500	
Major Cations	0.11	Na ≤ 50	Na > 50				NO <sub>3</sub> -N < 5.0	5.0 ≤ NO <sub>3</sub> -N ≤ 30.0	NO <sub>3</sub> -N > 30.0	
		Ca ≤ 75	Ca > 75				pH ≤ 8.0	6.5 ≤ pH < 7.0 and 8.0 < pH ≤ 8.5	pH < 6.5 or pH > 8.5	
Miscellaneous effect	0.05	Mg ≤ 30	Mg > 30							
		HCO <sub>3</sub> ≤ 300	HCO <sub>3</sub> > 300							
		K ≤ 10	K > 10							

Table 3. Judgment matrix of parameters for the evaluation of DWQI and IWQI.

Judgement matrix for DWQI								
	Toxic Metals	Toxic Anions	TDS & pH	Major Cations	Miscellaneous effect	Eigen vector	$\lambda$ max	Consistency ratio
Toxic Metals	1.00	1.50	2.00	3.00	5.00	0.35	5.14	0.03 < 0.1
Toxic Anions	0.67	1.00	1.50	3.00	5.00	0.27		
TDS & pH	0.50	0.67	1.00	3.00	5.00	0.22		
Major Cations	0.33	0.33	0.33	1.00	3.00	0.11		
Miscellaneous effect	0.20	0.20	0.20	0.33	1.00	0.05		

Judgement matrix for IWQI								
	Salinity	Permeability	Specific ion	Trace element	Miscellaneous effect	Eigen vector	$\lambda$ max	Consistency ratio
Salinity	1.00	1.20	5.00	7.00	9.00	0.43	5.35	0.08 < 0.1
Permeability	0.83	1.00	3.00	5.00	7.00	0.32		
Specific ion	0.20	0.33	1.00	3.00	5.00	0.14		
Trace element	0.14	0.33	0.33	1.00	2.00	0.07		
Miscellaneous effect	0.11	0.14	0.20	0.50	1.00	0.04		

standard limits. For DWQI, the quality rating of each physico-chemical parameter was given as 1 (unsuitable) or 2 (suitable). For IWQI, the rating of each physico-chemical parameter was given 1 (unsuitable) or 2 (moderately suitable) or 3 (highly suitable). Finally, the WQI was calculated through the equation (2).

$$WQI = \sum_{i=1}^N C_i, \tag{2}$$

where  $i$  is incremental index,  $N$  is number of category,  $C$  is score of each contributing category.

$C_i$  was calculated through the equation

$$C_i = (w_i) \times \frac{\left(\sum_{j=1}^n r_j\right)}{n}, \tag{3}$$

where  $w$  is the weightage value of the category,  $i$  and  $j$  are incremental index,  $r$  is rating of each water quality parameters,  $n$  is number of water quality parameters of the particular category.

The spatial distribution maps of WQI of the study area were prepared by surfer 9 software (golden software Inc., USA) using kriging method.

### 3.3 Saturation Index (SI)

SI is a measure of degree of equilibrium between water and respective minerals. It was calculated in the Phreeqc Interactive Software (Toran and Grandstaff 2002) using equation 4.

$$SI = \log\left(\frac{IAP}{Kt}\right), \tag{4}$$

where  $IAP$  is ion activity product and  $Kt$  is solubility product.  $SI$  value greater than zero indicates groundwater supersaturated with respect to the certain mineral; whereas  $SI$  value lesser than zero indicates undersaturation.

### 3.4 Groundwater flow modelling

The groundwater flow model of the study area was developed using Visual Modflow 2009.1. MODFLOW solves the partial differential equation describing the three-dimensional flow of groundwater in a heterogeneous porous medium by finite difference approximations (equation 5) (Harbaugh *et al.* 2000).

$$\frac{\partial}{\partial x} \left( K_{xx} \frac{\partial h}{\partial x} \right) + \frac{\partial}{\partial y} \left( K_{yy} \frac{\partial h}{\partial y} \right) + \frac{\partial}{\partial z} \left( K_{zz} \frac{\partial h}{\partial z} \right) - W = S_s \frac{\partial h}{\partial t}, \tag{5}$$

where  $K_{xx}$ ,  $K_{yy}$ ,  $K_{zz}$  are values of hydraulic conductivity along the x, y, and z directions;  $h$  is piezometric head;  $W$  is the volumetric flux of water per unit volume of aquifer representing sources and sinks;  $S_s$  is specific storage; and  $t$  is time.

Drain boundary is typically a head dependent boundary condition, which removes water from the aquifer at a rate proportional to the difference

between the head in the aquifer and some fixed head or elevation. It can be used in determining seepage rate from tunnels, springs (Anderson *et al.* 2015). Drain elevation and conductance value of seepage face were ascertained in drain boundary (equation 6).

$$Q = C\Delta h = C(h_B - h_{i,j,k}), \quad (6)$$

$$C = KA/L, \quad (7)$$

where  $\Delta h$  is the difference between the user-specified boundary head,  $h_B$ , and the model-calculated head near the boundary,  $h_{i,j,k}$ ;  $C$  is conductance ( $L^2/T$ ), which is computed using a representative hydraulic conductivity ( $K$ ) times a representative area ( $A$ ), divided by the distance ( $L$ ) between the locations of  $h_B$  and  $h_{i,j,k}$ . The given conductance value of the faces were user-specified. Blasting occurs in areas of excavations which may generate secondary porosity and greater permeability attributing high conductance to the layers. During modelling, a high value of conductance was assigned in the model (Peksezer-Sayit *et al.* 2014; Unsal and Yazicigil 2015). Model calculates inflow into the mine through saturated mine faces and upward flow from pit bottom.

## 4. Results and discussions

### 4.1 Groundwater quality

#### 4.1.1 Water quality analysis for drinking purpose

The distributions of seasonal concentration of major ions are shown in box plots (figure 2). As, Cd, Cr, Cu, Mn, Ni, Pb, Zn are found well below the desirable limits of drinking standards of BIS 2012 and WHO 1997. A comparative study of individual groundwater parameters with drinking water standards has been done. Table 4 elaborates the groundwater quality of the study area in both post- and pre-monsoon season in terms of percentage of groundwater samples for individual physico-chemical parameters. DWQI is used to observe the overall impacts of the physico-chemical parameters in groundwater for drinking purpose. All relevant established parameters having impact on water quality of particular use have been categorised into five subgroups and the weightage of each group is assigned according to

their impact on human health through AHP. The permissible limits of various heavy metals for drinking water are very low. Heavy metals are highly toxic to human health and is assigned highest weightage among the five groups. Toxic anions are getting second highest weightage among the groups, followed by TDS-pH and major cations. K and  $HCO_3$  are given lowest weightage (table 2). The DWQI is calculated through equation (2) and worked out into four categories (excellent, moderately suitable, poorly suitable and unsuitable) for drinking purpose (table 5). The result shows that most of the groundwater samples lie in the moderately suitable category and few lie in the excellent category of drinking purpose in both seasons. The spatial distribution maps of DWQI are prepared for both post- and pre-monsoon seasons show that the southern part of the study area comprises excellent water quality for drinking purpose (figure 3a and b).

#### 4.1.2 Suitability for irrigation, domestic and industrial purpose

Application of water with high concentration of Na increases the amount of sodium in soil and it replaces equivalent amount of calcium and other ions. As a result, it reduces permeability of soil and causes deflocculation. The application of calcium-rich water causes flocculation and increases permeability of soil (Todd and Myas 2005). In groundwater, calcium and magnesium normally sustain the equilibrium condition. Higher concentration of magnesium in water increases alkalinity of the soil and decreases the ability of crop yield. Table 6 classifies the groundwater suitability for irrigation, domestic and industrial purpose. SAR indicates that groundwater hold good irrigation quality in both post- and pre-monsoon seasons. RSC portrays the difference between total alkalinity and  $Ca + Mg$ . Results of RSC shows in post-monsoon 60.37%, 26.09% and 13.04% samples are safe, marginally suitable and unsuitable, respectively, whereas in pre-monsoon 66.67%, 14.58% and 18.75% samples are safe, marginally suitable and unsuitable, respectively. All samples are suitable for irrigation purpose with respect to MAR in post-monsoon; while 89.58% samples are suitable and 10.42% samples are unsuitable in pre-monsoon. KR is also used as an indicative parameter to see the suitability of



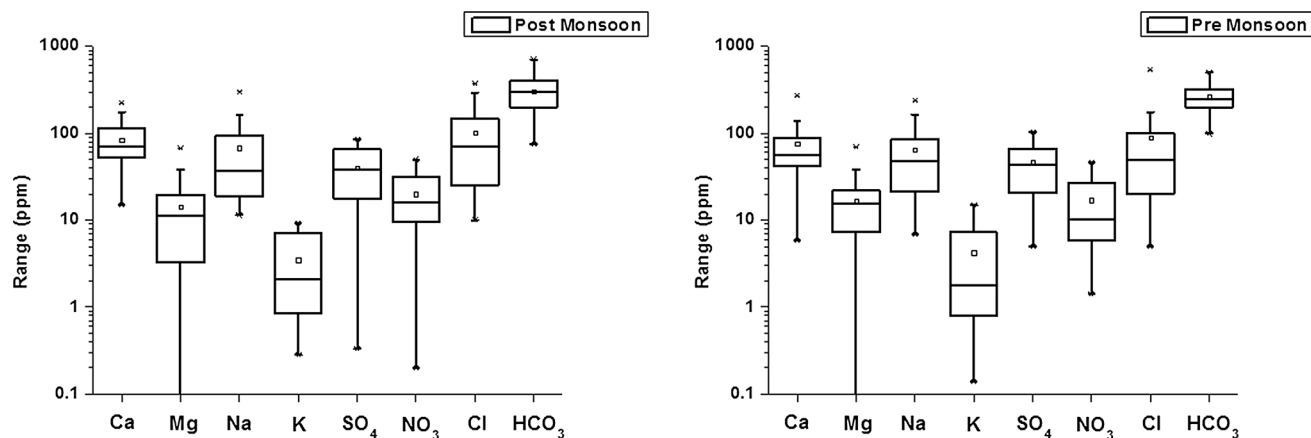


Figure 2. Box plots of major ions in pre-monsoon and post-monsoon seasons.

Table 4. Comparison of groundwater with drinking water standards, BIS (2012) and WHO (1997).

Chemical parameters	BIS (2012)		WHO (1997)			
	Acceptable limit	% of sample within acceptable limit		Acceptable limit	% of sample within acceptable limit	
		Post-monsoon	Pre-monsoon		Post-monsoon	Pre-monsoon
pH	6.5–8.5	65.22	100.00	7.0–8.0	4.35	68.75
TDS (ppm)	500	54.35	64.58	500	54.35	64.58
Ca (ppm)	75	56.52	62.50	75	56.52	62.50
Mg (ppm)	30	91.30	91.67	30	91.30	91.67
Na (ppm)	–	–	–	50	58.70	52.08
K (ppm)	–	–	–	10	100.00	83.33
SO <sub>4</sub> (ppm)	200	100.00	100.00	200	100.00	100.00
NO <sub>3</sub> (ppm)	45	95.65	95.83	50	100.00	100.00
Cl (ppm)	250	89.13	91.67	250	89.13	91.67
HCO <sub>3</sub> (ppm)	300	52.17	68.75	300	52.17	68.75
As (ppm)	0.01	100.00	100.00	0.01	100.00	100.00
Cd (ppm)	0.003	100.00	100.00	0.003	100.00	100.00
Cr (ppm)	0.05	100.00	100.00	–	–	–
Cu (ppm)	0.05	100.00	100.00	1	100.00	100.00
F (ppm)	1.5	2.17	100.00	–	–	–
Fe (ppm)	0.3	52.17	84.78	0.3	52.17	84.78
Mn (ppm)	0.1	100.00	100.00	0.1	100.00	100.00
Ni (ppm)	0.02	100.00	100.00	0.02	100.00	100.00
Pb (ppm)	0.01	100.00	100.00	0.01	100.00	100.00
Zn (ppm)	5	100.00	100.00	3	100.00	100.00

groundwater for irrigation purposes. According to KR, all pre-monsoon samples are found suitable for irrigation purpose. In post-monsoon season, 89.13% samples are found suitable and 10.87% samples are found unsuitable for irrigation purpose.

Permeability index (PI) diagram and Wilcox diagram are also used to test the groundwater suitability for irrigation purpose. PI is calculated using equation (8) and plotted against total ion

concentration in PI diagram (figure 4a and b). Diagram shows four samples of post-monsoon season and two samples of pre-monsoon season are in class III region, which are unsuitable for irrigation purpose. The scatter plot of Na% (calculated by equation 9) and electrical conductivity in Wilcox diagram (figure 4c and d) show two post-monsoon and three pre-monsoon samples are unsuitable for irrigation purpose.

Table 5. Categorization of WQI values.

WQI	Classifications	Range	Percentage of sample	
			Post-monsoon	Pre-monsoon
DWQI	Excellent	2	10.87	27.08
	Moderately suitable	$\geq 1.5$ to $< 2$	89.13	72.92
	Poorly suitable	$> 1$ to $< 1.5$	–	–
	Unsuitable	1	–	–
IWQI	Excellent	3	–	–
	Moderately suitable	$\geq 2$ to $< 3$	97.83	100
	Poorly suitable	$> 1$ to $< 2$	2.17	–
	Unsuitable	1	–	–

$$PI = \frac{Na + \sqrt{HCO_3}}{Ca + Mg + Na} \times 100, \quad (8)$$

$$Na\% = \frac{Na + K}{Ca + Mg + Na + K} \times 100. \quad (9)$$

Use of different indices/ratios sometime creates confusions like the result of one index may turn out as suitable for a particular use of groundwater and another index may turn out as unsuitable for the same use. Therefore, authors prefer single indexing procedures, which can assimilate all the allied parameters to take a decision. Five hazard groups namely (a) salinity hazard, (b) permeability hazard, (c) specific ion toxicity, (d) trace element toxicity, and (e) miscellaneous effect are considered to calculate the IWQI. Soils often lose its fertility due to salinity hazard. The salts (dissolved minerals) of applied irrigation water start to accumulate in the crop root zone of crop which restricts the availability of water to crop. Permeability hazard affect the soil by reducing the infiltration rate of irrigated water. Concentration of sodium, magnesium and calcium ions influence the permeability of soil. The influence of permeability hazard is measured through SAR, Na%. Ion like chloride has toxic effect on crops. It may cause leaf burn or leaf tissue. Generally, water with chloride  $< 140$  mg/l is considered good for irrigation purpose. Heavy metals and some trace elements in water cause soil pollution. They can resist biodegradation and thermo-degradation (Bohn *et al.* 2001). Plants take trace elements in their root system and accumulate in stems and leaves. This accretion affects plant growth and yield, which may cause plant to death. Consumption of unhealthy crops may have bio-magnification effect in the food chain. Effects of pH, alkalinity and nitrate on crops are taken as

miscellaneous problem. Acidic pH causes high concentration of heavy metals. It can influence carbonate equilibrium and relative ratio of nitrogen compounds, which adversely affect plant growth and soil quality. Alkaline water is suitable for uptake of several nutrients by plants. High alkalinity implies pH  $> 8.5$  in water. At very high pH, carbonates have tendency to form insoluble minerals, which leave behind the sodium ions in solution phase. High sodium affects soil fertility. Nitrate is the major source of nitrogen for plants, which help in plant growth. But excessive nitrate may adversely affect crop growth (Simsek and Gunduz 2007). All these parameters are categorised into five groups and the weightage is assigned according to their influence on irrigation potential (table 2). IWQI is calculated through equation (2). IWQI of  $\geq 2 < 3$  is considered as moderately suitable for irrigation purpose (table 5). The spatial distribution map of IWQI is shown in figure 3(c and d). The result displays that overall groundwater is suitable for irrigation purpose in both post- and pre-monsoon seasons. However, the IWQI  $< 2$  has been found at a place nearer to the OCCM during post-monsoon season. TDS and Na concentrations in post-monsoon season are quite high at few wells nearer to the OCCM, which affects IWQI strongly.

Corrosivity ratio (CR) is a measure of corrosive nature of water calculated by equation (10), where all the ions are expressed in ppm. CR  $> 1$  indicates corrosive nature of groundwater and transportation of water through any metallic pipe in industries or in domestic tube wells is unsafe (Majumdar *et al.* 2014; Das *et al.* 2016). 15.22% (post-monsoon) and 20% (pre-monsoon) samples possess CR  $< 1$ ; 84.78% (post-monsoon) and 79.97% (pre-monsoon) samples are showing CR  $> 1$ . Therefore, use of metallic pipe is very risky in this region.

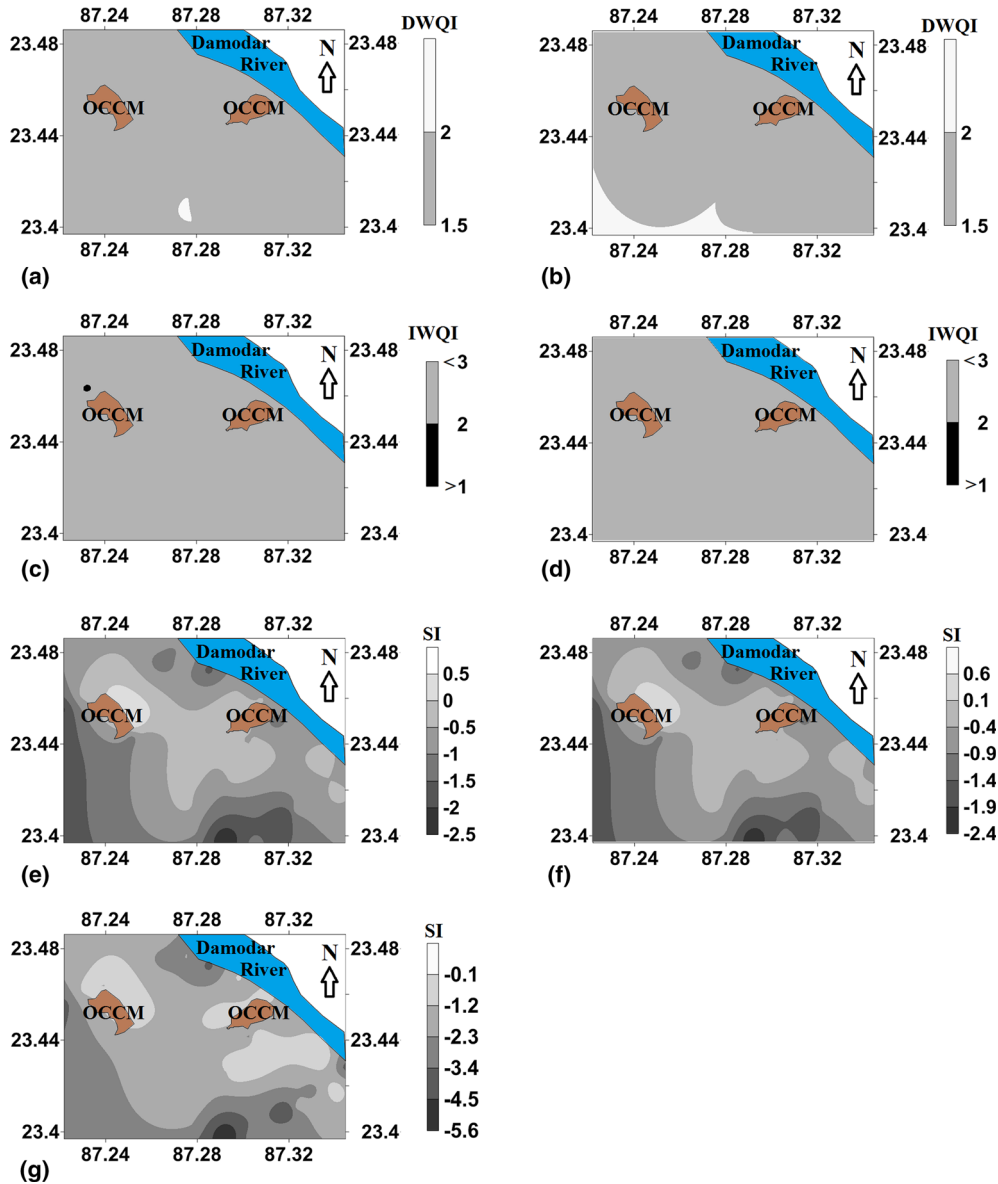


Figure 3. Indexed maps. (a) post-monsoon DWQI; (b) pre-monsoon DWQI; (c) post-monsoon IWQI; (d) pre-monsoon IWQI; (e) SI of aragonite; (f) SI of calcite; and (g) SI of dolomite.

$$CR = \frac{\left(\frac{Cl}{35.5}\right) + 2\left(\frac{SO_4}{96}\right)}{2\left(\frac{HCO_3 + CO_3}{100}\right)} \quad (10)$$

Total hardness (TH) of water is a parameter which helps to understand the suitability of water for domestic and industrial use. Hard water inhibits soap formation in water by precipitating calcium and/or magnesium salts of carbonates, sulphates and chlorides. It makes scaling in pipes, pot and boilers and may cause kidney failure and heart diseases. Hardness may be temporary or permanent. Temporary hardness generally indicates the occurrence of calcium carbonate and can be removed by boiling the water. On the other hand, permanent hardness is caused by the

existence of calcium, magnesium, chloride and sulphate ions. Ion exchange process is the only process which can remove it (Vasanthavigar *et al.* 2010). TH is calculated using the following equation (11) (Todd 1980):

$$TH = (2.497 \times Ca) + (4.115 \times Mg). \quad (11)$$

Among water samples of post-monsoon 4.5%, 17.39%, 47.83% and 30.43% belong to soft, moderate, hard and very hard category, respectively. TDS *vs.* TH plot (figure 4e) shows groundwater in this region is mainly hard fresh type in both post- and pre-monsoon season, whereas some samples are showing soft fresh nature and a little fraction shows hard brackish nature.

Table 6. Classification of groundwater quality based on water quality parameters.

Water quality parameters	Range	Class	Percentage of samples	
			Post-monsoon	Pre-monsoon
Sodium absorption ratio	< 6	Good	100.00	100.00
	6–9	Doubtful	–	–
	> 9	Unsuitable	–	–
Residual sodium carbonate	< 1.25	Safe	60.87	66.67
	1.25–2.50	Marginally suitable	26.09	14.58
	< 2.50	Unsuitable	13.04	18.75
Magnesium absorption ratio	< 50	Suitable	100.00	89.58
	> 50	Unsuitable	–	10.42
Kelly's ratio	< 1.0	Suitable	89.13	100.00
	> 1.0	Unsuitable	10.87	–
Corrosivity ratio	< 1	Suitable	15.22	20.83
	> 1	Unsuitable	84.78	79.17
Total hardness	< 75	Soft	4.35	4.17
	75–150	Moderate	17.39	22.92
	150–300	Hard	47.83	45.83
	> 300	Very hard	30.43	27.08

#### 4.2 Natural attenuation of AMD

Pyrite is a common mineral associated with coal mine spoils. Prolonged exposure of mine spoils in the surface environment creates AMD during rainy season. AMD causes lowering of pH and in turn percolating acidic water progressively become enriched with metal content including toxic heavy metals. However, the groundwater in the present study area is devoid of effect of AMD. Local hydro-geochemical reactions play key role in attenuation of AMD. The pH of AMD may get neutralized when it interact with carbonate minerals. Equiline diagrams are used in determination of prevailing hydro-geochemical processes in an area. The chemical equilibrium of carbonate minerals is calculated to evaluate the degree of saturation of these minerals in groundwater of the study area.

The scatter plots of (Ca + Mg) *vs.* (SO<sub>4</sub> + HCO<sub>3</sub>), (Na + K) *vs.* Cl are shown in figure 5. According to Rajmohan and Elango (2004), dissolution of calcite, dolomite and gypsum is the dominant reaction process, if plot of (Ca + Mg) *vs.* (SO<sub>4</sub> + HCO<sub>3</sub>) lie around the equiline line. Rina *et al.* (2011) suggests carbonate weathering is the dominant if samples lie above the equiline of (Ca + Mg) *vs.* (SO<sub>4</sub> + HCO<sub>3</sub>); whereas the ratio lying below the equiline signifies silicate weathering. Ratio of Na/Cl greater than one also indicates silicate weathering. Kim (2003) suggests that carbonate and silicate weathering reaction occurs

if ratio of alkalinity: Σcations falls around the equiline.

In present study, scatter plot of (Ca + Mg) *vs.* (SO<sub>4</sub> + HCO<sub>3</sub>) (figure 5a) shows 67.39% (post-monsoon) and 70.83% (pre-monsoon) samples fall below the equiline. However, 32.61% (post-monsoon) and 29.17% (pre-monsoon) samples lie above the equiline. Scatter plot of (Na + K) *vs.* Cl (figure 5b) shows that most of the samples in pre-monsoon (70.83%) lie above equiline. 68.75% pre-monsoon samples and 52.17% post-monsoon samples are found Na/Cl ratio > 1. It indicates carbonate and silicate weathering is the dominant process prevailing in both pre- and post-monsoon seasons.

The SI of anhydrite, aragonite, calcite, dolomite, gypsum, halite and siderite minerals are shown in table 7. Groundwater is at undersaturated condition in both post-monsoon and pre-monsoon seasons with respect to these minerals. However, degree of saturation is increased during pre-monsoon season. In monsoon season, groundwater recharge through precipitation causes dilution of groundwater; whereas in summer time, evaporation amplifies the degree of saturation. Spatial distribution map of SI of aragonite, calcite and dolomite minerals suggests that degree of saturation of these carbonate minerals has increased in places around the OCCMs (figure 3e–g). Aragonite and calcite are at supersaturated condition near the OCCMs. Dolomite shows undersaturated

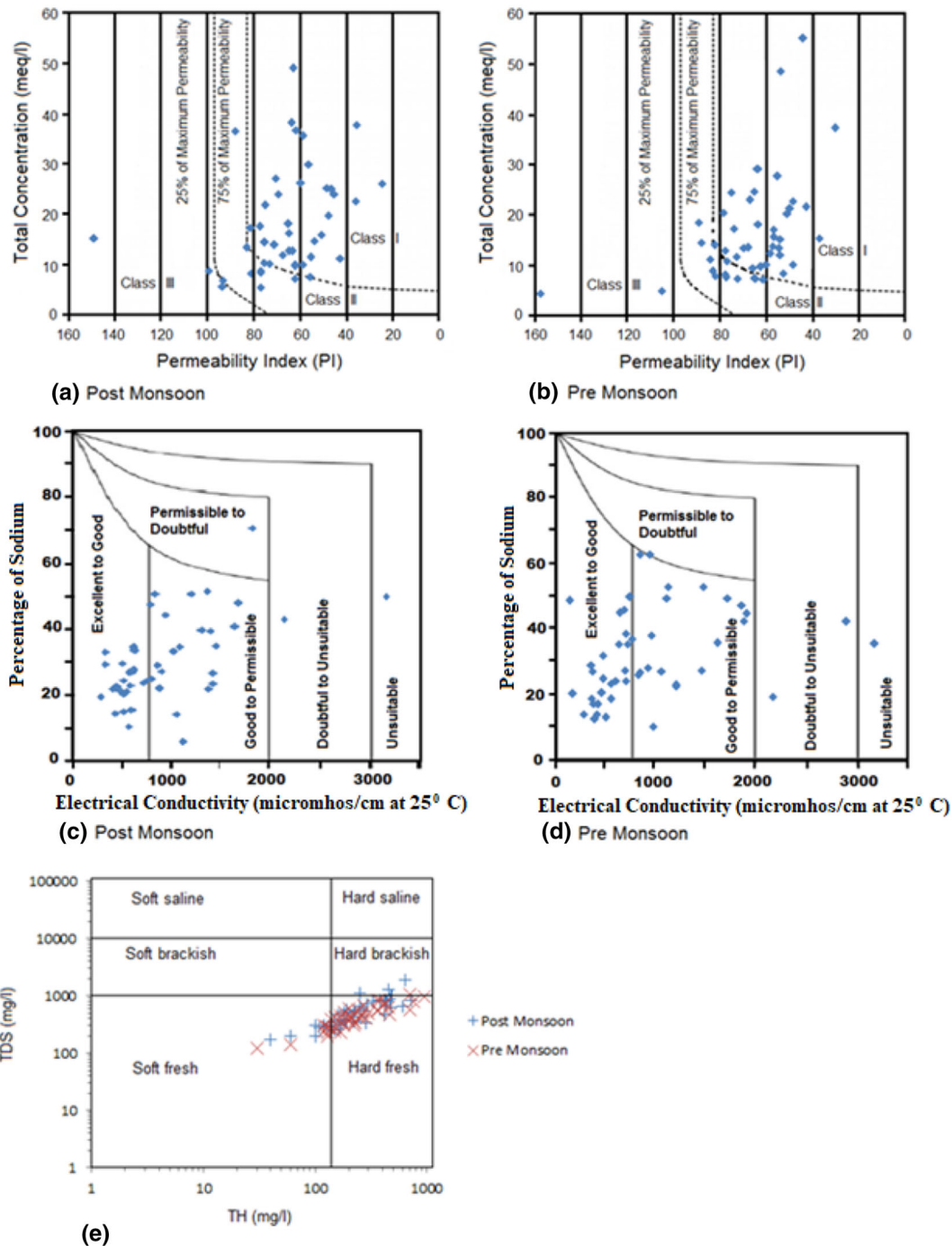


Figure 4. Permeability index (a and b), Wilcox (c and d) and (e) TDS vs. TH diagram of post-monsoon and pre-monsoon groundwater samples.

condition throughout the study area, but degree of saturation of dolomite is relatively higher in places close to the OCCMs. Carbonate minerals can act as buffering agent which reduces the effect of AMD in the study area. Reaction with carbonate minerals can neutralize pH of leachate and it may lead to adsorption and co-precipitation of various heavy metals with ferric and Al oxyhydroxides and sulphates (Flores and Sola 2010).

Further, the physico-chemical properties of soil (clay minerals, dissolved organic matter, cation exchange capacity, specific surface area, etc.) may play significant role in attenuation of contaminant in groundwater. Certain clay like montmorillonite (sodium clay) has very high cation exchange capacity (80 meq/100 gm) (Brady and Weil 2002), can interact with calcium concentrated water and make it sodium rich. Chloroalkaline



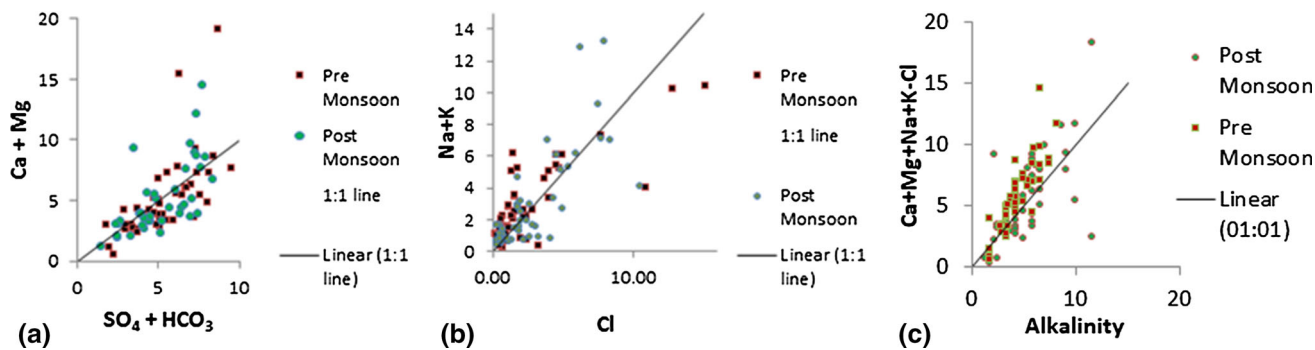


Figure 5. Equiline diagrams of post-monsoon and pre-monsoon groundwater samples.

Table 7. Calculated SI of anhydrite, aragonite, calcite, dolomite, gypsum, halite and siderite minerals in the study area.

Mineral phase	Season	Mean	Median	Minimum	Maximum
Anhydrite	Post-monsoon	-2.50	-2.32	-4.62	-1.76
	Pre-monsoon	-2.42	-2.37	-3.34	-1.56
Aragonite	Post-monsoon	-0.71	-0.59	-2.54	0.52
	Pre-monsoon	-0.22	-0.21	-2.05	0.64
Calcite	Post-monsoon	-0.56	-0.45	-2.40	0.67
	Pre-monsoon	-0.07	-0.07	-1.91	0.78
Dolomite	Post-monsoon	-1.74	-1.52	-5.71	-0.01
	Pre-monsoon	-0.52	-0.41	-4.31	1.20
Gypsum	Post-monsoon	-2.20	-2.02	-4.31	-1.46
	Pre-monsoon	-2.12	-2.07	-3.04	-1.25
Halite	Post-monsoon	-7.12	-7.13	-8.48	-5.70
	Pre-monsoon	-7.22	-7.20	-8.46	-5.53
Siderite	Post-monsoon	-1.13	-0.88	-4.86	0.64
	Pre-monsoon	-2.95	-3.92	-5.20	1.03

indices (CAI I and CAI II) are used to understand ion exchange behaviour of groundwater with the aquifer system. CAI I and CAI II are calculated by equations (12 and 13). Chloroalkaline indices can be positive or it can be negative. A positive value (direct exchange) indicates exchange of sodium and potassium of water with calcium and magnesium of rocks; whereas negative value (reverse exchange) indicates exchange of calcium and magnesium of water with sodium and potassium of rocks (Adhikari *et al.* 2013). In post-monsoon season, 58.70% samples are showing negative value and 41.30% samples are showing positive value; whereas in pre-monsoon, 70.83% samples are showing negative value and 29.17% samples are showing positive value. Therefore, sodium and potassium of rocks are dominantly replacing the calcium and magnesium from groundwater during

pre-monsoon; however, this ion exchange pattern is not same in post-monsoon. During post-monsoon both direct and reverse process of ion exchange occurs.

$$\text{CAI - I} = \frac{\text{Cl} - (\text{Na} + \text{K})}{\text{Cl}} \quad (12)$$

$$\text{CAI - II} = \frac{\text{Cl} - (\text{Na} + \text{K})}{\text{SO}_4 + \text{HCO}_3 + \text{CO}_3 + \text{NO}_3}. \quad (13)$$

All this hydro-geochemical processes occurring in the study area, affect the overall groundwater quality in both post- and pre-monsoon seasons. In post-monsoon, groundwater is mainly Ca-HCO<sub>3</sub> type; a few samples are showing Ca-Na+K-Mg-HCO<sub>3</sub> type. In pre-monsoon season, groundwater shows mainly Ca-Na+K-Mg-HCO<sub>3</sub> type.

### 4.3 Groundwater flow model

#### 4.3.1 Conceptual model

Prior to decipher any site-specific groundwater problem, there should have a clear knowledge about key features which portray the groundwater system such as horizontal and vertical disposition of various geological materials, groundwater flow pattern, recharge of groundwater through precipitation as well as from surface water sources, natural discharge and pumping of groundwater. During excavation, inflow into the mine occurs through saturated mine faces exposed in the profile and from pit bottom (figure 6a).

Figure 6(c) shows progressive development of OCCM 2 from 2011 to 2016. The satellite images were obtained from historic imagery option of Google earth. The mining operation started in 2011 and continued till 2014. After 2014, the mining operation has been stopped due to legislative problem. At present OCCM 2 is not in operating condition. Groundwater was pumped out till 2014 for safe mining operation and after that pumping operation has been stopped. Consequently, ponding of groundwater started since 2015 (figure 6c). It is essential to have water table data of pre-mining and during mining to assess the inflow of groundwater into the mine and impact of dewatering on the surrounding aquifers. The water table data from 1996 to 2017 were studied in four observation wells namely OB1, OB2, OB3 and OB 4 (figure 6e) to observe the effect of mining. Figure 6(d) shows fluctuations of water table in the four observation wells over time. Water table declined sharply in 2011 at OB2 which is in close proximity to the mine site; whereas no such significant variation was observed in other wells away from the mine. Groundwater in the surrounding region of mine is under threat of declination of water table. Study area consists of various lithological units. Different lithologic units possess different hydrogeological properties. Thus, mine will receive different rate of inflow through different hydro-geologic units exposed during the vertical enhancement of the excavation. Based on the available data of the study area, subsurface dispositions of six hydrogeological layers were conceptualized. General lithological column (figure 6b) of the mined area shows the presence of two mineable coal seams in this region. Coal Seam II, situated at depth 12–2 m from msl, is thicker than Coal Seam I. Coal Seam I is situated at greater depth. Furthermore,

Gondwana, being a rift basin, is made up of large and small scale fault structures. The spatial disposition of these coal layers differ due to dip of the beds and presence of fault (figure 6b). As Gondwana beds are very gently dipping ( $0-5^\circ$ ), depth variation of a strata within a short horizontal distance should be small. Greater vertical shift of strata within short horizontal distance indicates the presence of fault. Greater vertical disposition of coal Seam I and Seam II within short lateral span towards north of the study area establishes the presence of fault. Therefore, depth of excavation in different stages of mine development will differ according to the disposition of the coal seams. Three stages of mine development were assigned in the model for better understanding of the effect of mine on hydrological sources (figure 6e). Stage 0 represents pre-mining condition, where no excavation was done. Stage 1 represents present mining condition where mine floor is situated at depth  $-30$  m from msl with an areal extension of  $0.33$  km<sup>2</sup>. In stage 2, mine is extrapolated according to the disposition of the coal layers, where the areal extension of the mine is  $2.03$  km<sup>2</sup> with a maximum mine floor depth of  $-122$  m from msl (base of coal Seam I).

The Damodar River is flowing from north-west to south-east direction. Durgapur barrage is situated in the northern part of the study area which store water for domestic and industrial purposes. An irrigation canal, originating from Durgapur Barrage, is passing through the study area (figure 1). These surface water bodies may act as source of groundwater recharge apart from rainfall. Groundwater pumping for domestic use and pumping of ponded groundwater seepage into the mine excavation are the main abstractions in the study area.

#### 4.3.2 Input model properties and boundary conditions

The model domain covered an area of  $50$  km<sup>2</sup>. The domain was divided into 100 rows and 50 columns, where individual cell covers  $100 \times 100$  m<sup>2</sup> area. The model top had a height of  $90$  m from msl and its bottom was fixed at  $-150$  m from msl. A relatively large grid pattern was assigned to the model. Large grid spacing generally cuts the small scale inhomogeneity of the aquifer. The surface of the study area mainly consists of fine to medium grained sandy deposits with sporadic clay. The model was vertically

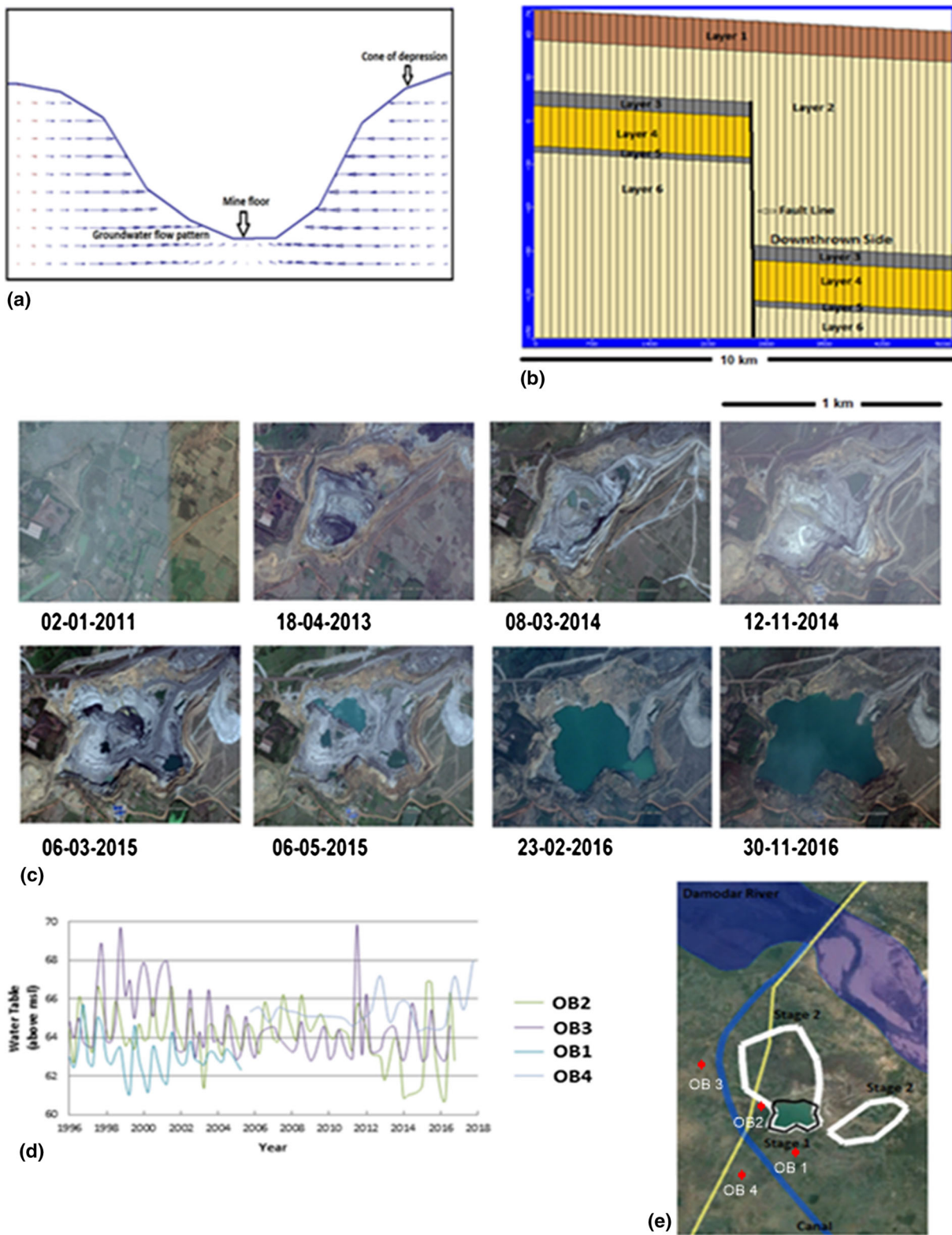


Figure 6. Conceptualization of the model area. (a) Conceptualization of groundwater inflow into mine; (b) E–W section of the model domain showing effect of fault in model geometry; (c) Progressive development of OCCM 2; (d) Water table fluctuation in four observation wells over years; (e) Stage of development of the mine.

divided into six hydrogeologic layers (figure 5b). Hydraulic conductivity and specific yield of various layers are tabulated in table 8 (Zheng and Bennett

2002). Layers are gently dipping towards north-east (Das *et al.* 1992; Roy and Ghosh 2002). Presence of faults in the study area made considerable disposition

Table 8. Hydraulic conductivity and specific yield of various layers.

Hydrogeological layers	HC (m/s)		Specific yield	
	Initial	Calibrated	Initial	Calibrated
Loose sand and clay intercalated layer (Layer 1)	$5 \times 10^{-4}$	$5 \times 10^{-5}$	0.28	0.2
Sandstone with few thin shale layers (Layer 2)	$6 \times 10^{-6}$	$2 \times 10^{-7}$	0.21	0.18
Coal seam II (Layer 3)	$1 \times 10^{-10}$	$1 \times 10^{-10}$	0.01	0.01
Sandstone and shale intercalated layer (Layer 4)	$6 \times 10^{-6}$	$2 \times 10^{-7}$	0.21	0.18
Coal seam I (Layer 5)	$1 \times 10^{-10}$	$1 \times 10^{-10}$	0.01	0.01
Sandstone (Layer 6)	$6 \times 10^{-6}$	$2 \times 10^{-7}$	0.21	0.18

of layers, except layer1. The effect of fault was assigned in model geometry through specifying the bottom elevation of each affected layer (figure 6b). Ground elevation near the mine site of the study area has been observed between 66 and 68 m from msl. During modelling, all the elevations were standardized with respect to msl. The study area receives average annual rainfall of 1204.5 mm. The maximum rain fall occurs in rainy season, i.e., from middle of June to middle of September. No field level study was done to estimate recharge of groundwater from precipitation. However, studies of groundwater resource estimation committee (1997) suggests 20–25% recharge occurs in alluvial terrain. Upper part of the study area being made up of sandy soil and loose sand of alluvium sequence, favours substantial infiltration. The components of precipitation have been split into 20% infiltration, 60% evapotranspiration and 20% surface runoff for the study area. Accordingly, the recharge from precipitation 252 mm/year was assigned to the model. The evapotranspiration of 756 mm and 2 m extinction depth (Shah *et al.* 2007) was assigned as evapotranspiration boundary condition. Keeping in view, the direction of regional groundwater flow (north to north-east), inflow of groundwater through southern and western boundaries into the model domain from outside the model area was considered as constant head mode. The head values in constant head boundaries were assigned from the water table contour map (Adhikari and Mal 2019). The Damodar River was assigned as river boundary in the model. Durgapur barrage across Damodar River was constructed in 1955. The water level in barrage lies in the range of 64.5–63.4 m from msl. The stored water is used for domestic, irrigation and industrial purposes. There is a stage difference between upstream side (64.5 m from msl) and downstream side (58 m from msl) at the barrage. The river bed in Damodar River is almost 12 m thick with assigned conductivity of 0.0002 m/s (Todd and Mays 2005; ECL Report 2015; Lathashri *et al.* 2016). The

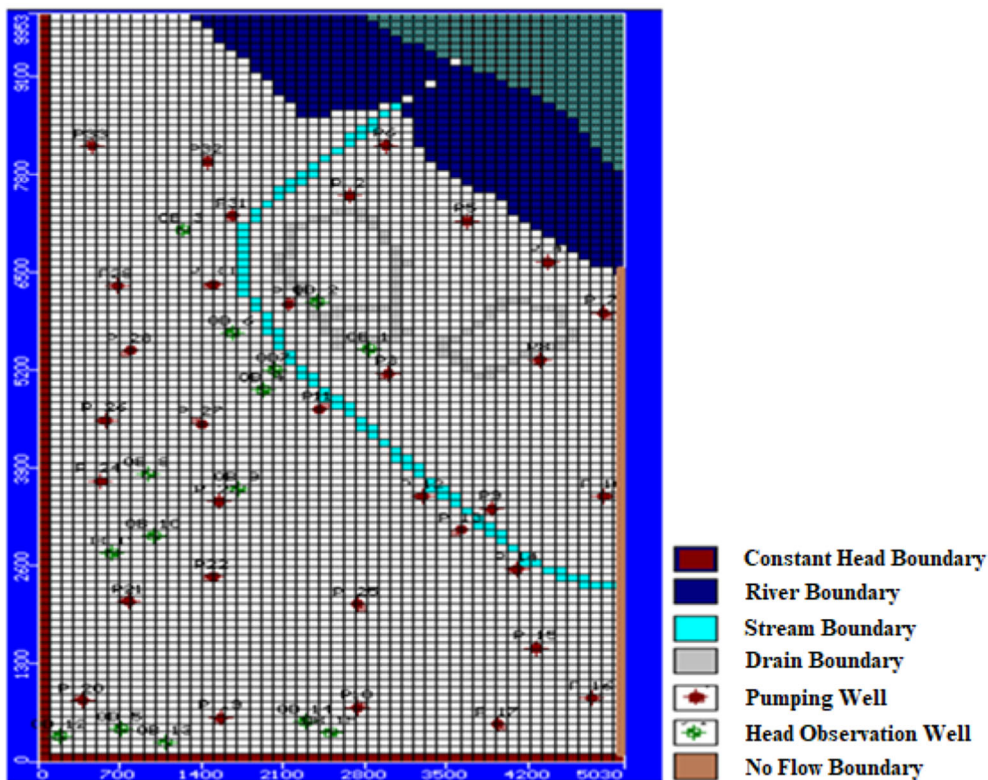
irrigation canal in the study area was assigned as stream boundary in the model domain. The canal has an average width of 15 m throughout the study area. The inflow into the stream was 64.3 cumec (<http://www.dvc.gov.in/activitiesdamsbarrages.htm>). The thickness of the stream bed was considered 1 m with conductivity of 0.0002 m/s. The eastern part of the model domain was assigned as no flow boundary. Groundwater withdrawal for domestic use has been calculated on the basis of population census data, 2011 and per capita consumption 50 liter/day. The withdrawal of groundwater for domestic use was assigned in the model through 33 pumping wells (figure 7a). Drain boundary was applied to the mine excavations.

#### 4.3.3 Model simulation

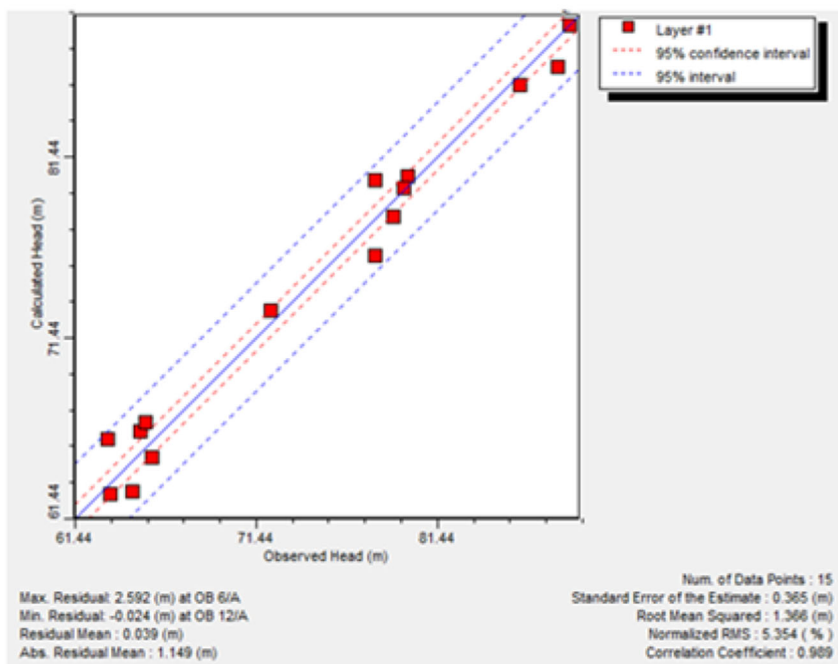
Numerical solutions were obtained using GMG (Wilson and Naff 2004) solver of MODFLOW-2000 (Harbaugh *et al.* 2000). Layer 1 was assigned as unconfined aquifer, whereas other water bearing layers were treated as confined aquifer in the layer setting window of MODFLOW. Arithmetic mean interblock transmissivity was applied to all the layers to calculate MODFLOW interface transmissivity. All the converging solutions resulted in discrepancies of < 0.1% in the flow budget.

First, the model was run under steady state condition. The hydraulic conductivity and initial boundary conditions were adjusted (table 8) during model calibration using trial and error method to match model predicted value with the field observed water level and flux data. In transient condition, specific storage and specific yield were adjusted and fixed to match observed flux data into the mine. The pre-mining condition (1996–2011) was retrieved through calibration of the model by water table data of four wells, obtained from





(a)



(b)

Figure 7. Boundary conditions (a) and calibration curve (b) of the model.

Central Groundwater Board of India (CGWB) and State Water Investigation Department of West Bengal (SWID). Further, the model was validated

with present data collected during fieldwork by the authors. Figure 7(b) shows the calibration curve of model predicted data and field measured data of



Table 9. Sensitivity analysis.

Parameter	Change	Drain value
Hydraulic conductivity	50% increased	38.37% increased
	50% decreased	52.42% decreased
	25% increased	19.26% increased
	25% decreased	19.40% decreased
Recharge through precipitation	50% increased	12.34% increased
	50% decreased	12.41% decreased
	25% increased	6.19% increased
	25% decreased	6.18% decreased
Constant head (as lateral inflow)	5 m increased	No change
	5 m decreased	0.05% decreased

observation wells. The calibration results with root mean square error (RMSE) of 1.36 m, normalized RMSE of 5.354% and correlation coefficient of 0.989, strongly vouch for the capability of the model to simulate the practical field condition.

#### 4.3.4 Sensitivity analysis

Sensitivity is a measure of the effect of change of one parameter on the changes of other parameters. Sensitivity analysis is needed especially when a model is calibrated through trial and error method. It is very useful in the study of effect of input parameters (like hydraulic conductivity, recharge, etc.) in a simulated model. It shows the difference of approximation of the dependable variable (mine inflow) by any change in model input parameters. Thus, it helps in identifying certain parameters which has high impact or negligible impact on the model.

The sensitivity analysis was performed using different recharge rates through variation of precipitation, hydraulic conductivity of the layers and constant head at the boundaries in stage 1 condition of mine development. Study area receives various rate of precipitation during different seasons in a year. Therefore, in the analysis of model uncertainty, recharge through precipitation increased and decreased up to 50% within a year. Heterogeneity of different water bearing layers ensued sensitivity check of hydraulic conductivity values up to 50% increase and decrease in the model. The model area is a small hydro-geological domain of a big groundwater basin. Lateral inflow in the model domain plays a vital role to the groundwater budget of the area. Water table fluctuation (figure 6d) shows maximum fluctuations at the southern and western parts of the model area. Whereas in northern part, nearer to the canal the

water table fluctuation was less. Constant head at the boundaries which represent the lateral inflow to the model were changed to  $\pm 5$  m from the model calibrated value. No significant change in mine seepage was observed due to change in constant head boundaries. Table 9 shows the result of the sensitivity analysis. It shows that the hydraulic conductivity is the main parameter which affects the seepage into the mine. Recharge through precipitation also plays important role in groundwater seepage at the mine.

#### 4.3.5 Assessment of dewatering impacts on local hydrology

Model at stage 0 was run in transient condition without any drain boundary condition. At stage 1 and stage 2 condition, drain boundary conditions were applied into the model. The model was calibrated according to the field observed water level and mine inflow data in transient condition. The simulations were done in monthly stress periods, with 10 time steps in each stress periods and with a multiplier of 1.2. Numerical modelling in transient condition accomplished changes in boundary conditions (seasonal precipitation, progressive mining with complex excavation geometry). During enhancement of mine, the model was run in transient condition for 10 years. The ratio of horizontal to vertical hydraulic conductivity was set 10:1 for all layers, except in regions of faults, where it was set 2:1 (Unsal and Yazicigil 2015). The recharge through precipitation and evapotranspiration, values were assigned in month-wise pattern using recharge and evapotranspiration boundary conditions, respectively. Mine progress in different development stages was defined using drain boundary condition in a time-wise manner by assigning drain elevation into the drain cells. The

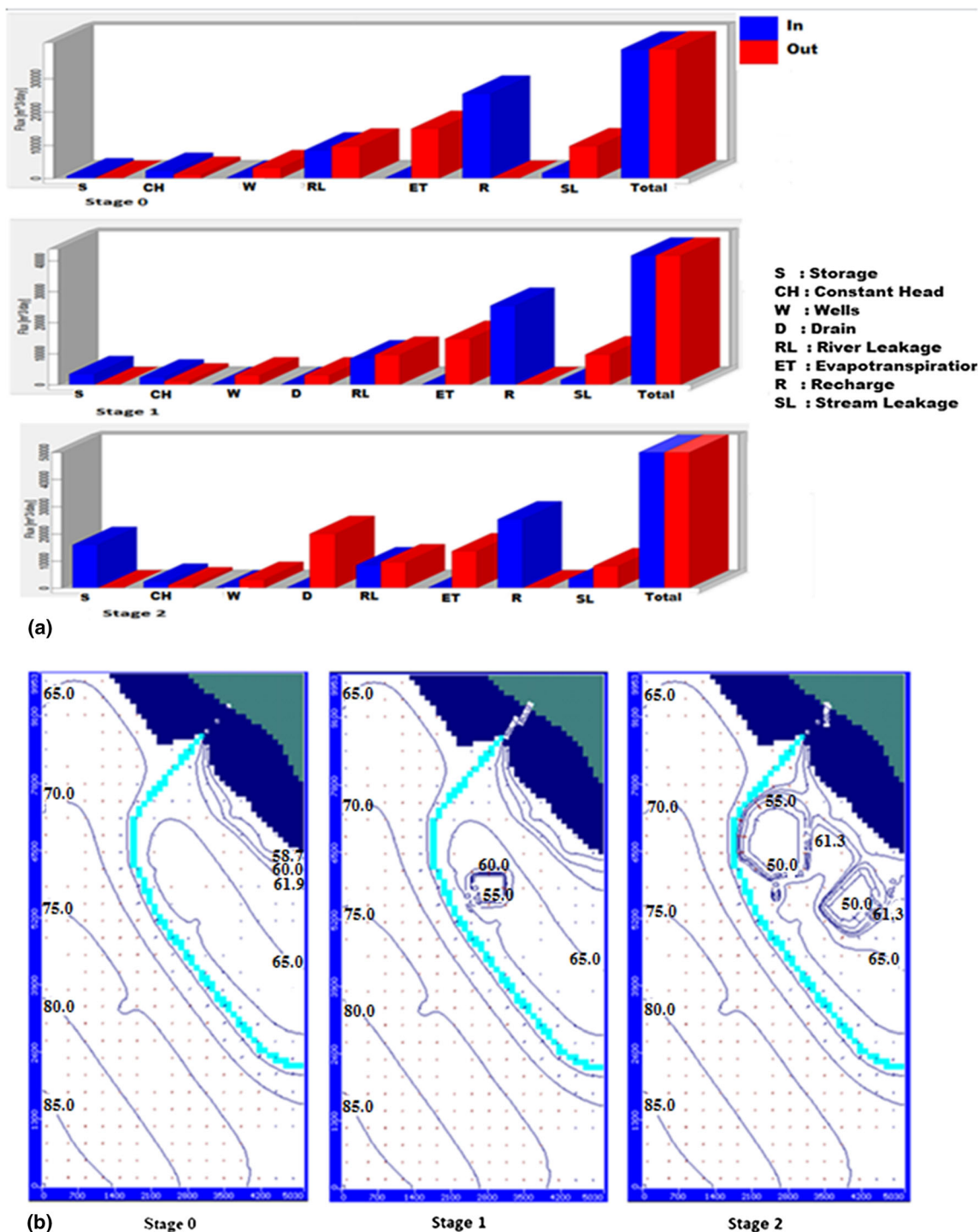


Figure 8. Groundwater budget (a) and distribution of head equipotential lines (b) in the study area at different stages.

groundwater budget and distribution of head equipotential lines in the study area at different stages are portrayed in figure 8.

No mining operation was simulated in stage 0 of model. The model was run in transient condition with calibrated input parameters for 10 years without drain boundary condition. The groundwater budget and groundwater flow pattern evaluated

during this stage (figure 8), display a north to north-east directional regional groundwater flow pattern in the study area. Groundwater basically feeds the Damodar River and irrigational canal (effluent stream) except in areas close to barrage, where river is recharging groundwater system.

At stage 1 condition, the floor of the mine was situated at -30 m from msl with an areal extent of

0.33 km<sup>2</sup> (figure 6e). Since the beginning of mining operation in 2011 till the operation stopped in 2014, the excavation covered an area of 0.33 km<sup>2</sup>. Vertically the stratum is divided into six layers. Different layers contribute different rate of inflow into the mine. The top layer among six water bearing layers consisting of soil, intercalation of clay and loose sand up to a depth of 21 m constitute main aquifer body in this region. It is an unconfined aquifer and contributes major seepage into the mine. People withdraw water from this layer for domestic use. Therefore, seepage from this aquifer will affect most to the local people. The drawdown in local groundwater table further affects surface water resources. Surface water may become influent in relation to the groundwater of the study area. The model does not show any appreciable effect of groundwater seepage on the surface water bodies at this stage. The surface water bodies were situated at greater distance from the present excavation site and the areal extension of the excavation at stage 1 was not so large. Thus, the influence of drawdown does not reach to the base of the surface water bodies. A small scale water table drawdown was observed around the mine site. The loss of groundwater through drain boundary increases the inflow into the storage of the aquifer system. Currently, mining operation is ceased due to legislative problem and the water table in the excavation site is reached to the equilibrium condition. But in future extension of mine, again the equilibrium condition of the local groundwater system will disrupt. The effect of seepage into the mine can be observed on surface water bodies if excavation occurs in close proximities of the surface water bodies.

In stage 2, the mine had been extended in north-west and north-east direction following the disposition of coal seams. The effect of fault on coal seam does not appear in north-west direction, but the depths of coal seams were increased due to the dip of the coal beds. In north-west direction, the pit bottom elevation was lowered and reached up to -56 m from msl with an areal extent of 1.55 km<sup>2</sup> (figure 6e). According to model prediction, mine receives groundwater inflow of 11,798 m<sup>3</sup>/d during this phase. As the excavation takes place close to the irrigation canal passing through this region, seepage to excavation causes leakage of water from the irrigation canal. Model estimated that stream will lose almost 1473 m<sup>3</sup>/d of water from its discharge through a stretch of ~1.7 km, which is close to the excavation site. Subsurface

geology in north-eastern part of the study area had been restructured through fault plane. The effect of fault had been observed on coal seams. Coal Seam II occurs at elevation of -86 m from msl and coal Seam I is found at -122 m from msl. During extension of the mine in north-eastern side of the study area, drain elevation was assigned -122 m into the model with an areal extent of 0.43 km<sup>2</sup> (figure 6e). The effect of fault does not appear in layer 1 (figure 6b). Model predicts inflow of 12,365 m<sup>3</sup>/d into mine cavity during stage 2. No significant loss of water from irrigation canal was observed during enhancement of mine in north-eastern direction. Water loss from canal occurs if the mine was extended in north-west direction. Further, model shows Damodar River will flow at its natural condition, no significant leakage from river will arise due to mining.

Apart from groundwater inflow, mine will receive water direct from precipitation. The average annual rainfall is 1204.5 mm/year and evapotranspiration is considered 756 mm/year. Therefore, mine receives 910,455 m<sup>3</sup>/year of water from rain in an excavation of 2.03 km<sup>2</sup>.

## 5. Conclusions

The impact of OCCMs on groundwater resources has been evaluated on the aspect of water quality and water budget. The following conclusions can be drawn from the present study:

- In lieu of individual application of different diagrams and indices, use of WQI is far more convenient to define the water quality as a whole with respect to specific use. The assigned relative weightage of various parameters of DWQI and IWQI were found good (consistency ratio of 0.03 and 0.08 for DWQI and IWQI, respectively) to evaluate WQI for drinking and irrigation purpose. The spatial distribution map of DWQI and IWQI specifies groundwater in this region is overall suitable for drinking and irrigation purpose with an exception of water from wells in close proximity of the OCCMs. The estimated value of several indices (SAR, RSC, MAR and KR) and plot of different diagrams (Wilcox and Permeability Index) conform the applicability and precision of present IWQI method.
- Overall rock-water interaction is the key process affecting groundwater geochemistry in both pre- and post-monsoon seasons. Plot of equiline

diagrams indicate that silicate and carbonate weathering are the dominant weathering process influencing groundwater chemistry. Effect of AMD is not observed in the study area. SI of carbonate minerals indicates that the groundwater in close proximity of OCCMs is supersaturated with respect to aragonite and calcite. These minerals may buffer the pH of AMD which renders adsorption and precipitation of various metals in the soil/rock and consequently resist the transport of many toxic metals to the groundwater. Lower Gondwana coal mines of other areas with similar rock association may also be free from AMD menace because of same self-natural buffer mechanism.

- Groundwater flow model provided a significant idea about the groundwater budget in the study area. Model predicts that in the stage 1 and 2, groundwater seepage into the mine will be 3120.6 and 24,163 m<sup>3</sup>/d, respectively. Water loss from the aquifer will cause lowering of water table in the surrounding areas of mine. Well (OB2) close to OCCM 2 with lowering of water table from 2011 to 2014 during operating stages of mine substantiates the negative impact of mining and associated dewatering process on the aquifer. Model predicted 4–5 m lowering of water table around 2.86 km<sup>2</sup> area of the mine cavity within 15 years. The irrigational canal may lose water of 1473 m<sup>3</sup>/d from its stream inflow on enhancement of mine in north-west direction, which may impact the production of agricultural crops in downstream areas. Present mining operation will not impact much on the flow condition of the Damodar River.

The detailed insight presented by this study may help for better hydrological management, if the mine starts operation in future.

### Acknowledgement

Authors acknowledge Department of Earth and Environmental Studies, National Institute of Technology Durgapur for the laboratory support.

### Author statement

Ujjal Mal carried out the field study, analysed samples and performed experiments and numerical modelling under the supervision of Kalyan

Adhikari. Ujjal Mal wrote the draft manuscript, which was modified by Kalyan Adhikari.

### References

- Adhikari K and Mal U 2019 Application of multivariate statistics in the analysis of groundwater geochemistry in and around the open cast coal mines of Barjora block, Bankura district, West Bengal, India; *Environ. Earth Sci.* **78** 72, <https://doi.org/10.1007/s12665-019-8071-0>.
- Adhikari K, Sadhu K, Chakroborty B and Gangopadhyay A 2013 Effect of mining on geochemistry of groundwater in Permocarboniferous Gondwana coalfields: Raniganj Basin, India; *J. Geol. Soc. India* **82** 392–402.
- Adhikari K, Chakroborty B and Gangopadhyay A 2012 Assessment of irrigation potential of groundwater using water quality index tool; *Environ. Res. J.* **6**(3) 197–205.
- Anderson M P and Woessner W W 1992 *Applied groundwater modeling*; Academic, San Diego.
- Anderson M P, Woessner W W and Hunt R J 2015 *Applied groundwater modeling*; 2nd edn, Academic, San Diego.
- APHA 1995 *Standard methods for the examination of water and waste water*; Washington: 19th edn, American Public Health Association, Washington, DC.
- Ardejani F D, Singh R N, Baafi E and Porter I 2003 A finite element model to: 1. Predict groundwater inflow to surface mining excavations; *Mine Water Environ.* **22**(1) 31–38.
- Aryafar A, Ardejani F D and Singh R N 2009 Numerical modeling of groundwater inflow from a confined aquifer into Sangan open pit mine, north-east Iran; *Geomech. Geoengin. Int. J.* **4**(3) 189–199.
- Bhowmick P and Ghosh J K 2002 Final report on regional exploration for coal in Mohanpur Sector, Raniganj Coalfield, Bankura District, West Bengal; Coal Wing, Geological Survey of India, [http://www.portal.gsi.gov.in/gsiDoc/fspReports/CW/1995-2000/CW\\_CWPR02879\\_1998\\_2000\\_REPORT\\_1.pdf](http://www.portal.gsi.gov.in/gsiDoc/fspReports/CW/1995-2000/CW_CWPR02879_1998_2000_REPORT_1.pdf).
- BIS 2012 Indian standard drinking water – specification (2nd revision), IS 10500:2012, Bureau of Indian Standards; <http://cgwb.gov.in/Documents/WQ-standards.pdf>.
- Bochenska T, Fiszler J and Kalisz M 2000 Prediction of groundwater inflow into copper mines of Lubin Glogow Copper District; *Environ. Geol.* **39**(6) 587–594.
- Bohn H L, McNeal B L and O'Connor G A 2001 *Soil chemistry*; 3rd edn, Wiley, New York, 320p.
- Brady N C and Weil R R 2002 *The Nature and Properties of Soils*; Prentice Hall: Upper Saddle River, NJ, 960p.
- Brouyere S, Orban P H, Wildemeersch S, Couturier J, Gardin N and Dassargues A 2009 The hybrid finite element mixing cell method: A new flexible method for modeling mine groundwater problems; *Mine Water Environ.* **28**(2) 102–114.
- Das P K, Bhattacharya T K and Bhowmick P 1992 Final Report on the Scout Boreholes Drilled in Trans-Damodar Sector, Raniganj Coalfield, Bankura District West Bengal; Coal Wing, Geological Survey of India; [http://www.portal.gsi.gov.in/gsiDoc/fspReports/CW/1985-1990/CW\\_CWPR\\_02454\\_1986\\_1990\\_REPORT\\_1.pdf](http://www.portal.gsi.gov.in/gsiDoc/fspReports/CW/1985-1990/CW_CWPR_02454_1986_1990_REPORT_1.pdf).
- Das P P, Sahoo H K and Mohapatra P P 2016 Hydrogeochemical evolution and potability evaluation of saline contaminated coastal aquifer system of Rajnagar, Odisha,



- India: A geospatial perspective; *J. Earth Syst. Sci.* **125**(6) 1157–1174, <https://doi.org/10.1007/s12040-016-0721-y>.
- Dhakate R, Modi D and Gurnadha Rao V V S 2019 Impact assessment of coal mining on river water and groundwater and its interaction through hydrological, isotopic characteristics, and simulation flow modeling; *Arab. J. Geosci.* **12** 8, <https://doi.org/10.1007/s12517-018-4110-5>.
- ECL Report 2015 Composite plan of sand mining in the riverbed of Damodar River; <http://environmentclearance.nic.in/writereaddata/EIA/11092015VCTO3EJ3empmin.pdf.pdf>.
- Flores A N and Sola F M 2010 Evaluation of metal attenuation from mine tailings in SE Spain (Sierra Almagrera): A soil-leaching column study; *Mine Water Environ.* **29** 53–67, <https://doi.org/10.1007/s10230-010-0099-z>.
- Fontaine R C, Davis A and Fennemore G G 2003 The comprehensive realistic yearly pi transient infilling code (CRYPTIC): A novel pit lake analytical solution; *Mine Water Environ.* **22**(4) 187–193.
- Gebrehiwot A B, Tadesse N and Jigar E 2011 Application of water quality index to assess suitability of groundwater quality for drinking purposes in Hantebet watershed. Tigray, Northern Ethiopia; *ISABB J. Food Agr. Sci.* **1** 22–30.
- GEC 1997 Groundwater resource estimation methodology; Report of the Groundwater Resource Estimation Committee, Ministry of Water Resources, Government of India, New Delhi.
- Harbaugh A W, Banta E R, Hill M C and McDonald M G 2000 MODFLOW-2000, U.S. Geological Survey modular ground-water model: User guide to modularization concepts and the groundwater flow processes; USGS Open file Report 00-92, Washington DC, USA.
- Jiang S, Kong X, Ye H and Zhou N 2013 Groundwater dewatering optimization in the Shengli no. 1 open-pit coalmine, Inner Mongolia, China; *Environ. Earth Sci.* **69** 187–196, <https://doi.org/10.1007/s12665-012-1946-y>.
- Kim K 2003 Long-term disturbance of ground water chemistry following well installation; *Groundwater* **41** 780–789.
- Kumar S K, Logeshkumaran A, Magesh N S, Godson P S and Chandrasekar N 2015 Hydro-geochemistry and application of water quality index (WQI) for groundwater quality assessment, Anna Nagar, part of Chennai City, Tamil Nadu, India; *Appl. Water Sci.* **5** 335–343, <https://doi.org/10.1007/s13201-014-0196-4>.
- Lathashri U A and Mahesha A 2016 Groundwater sustainability assessment in coastal aquifers; *J. Earth Syst. Sci.* **125**(6) 1103–1118, <https://doi.org/10.1007/s12040-016-0719-5>.
- Low K S, Lee G K and Liew S C 2000 Sorption of cadmium and lead from aqueous solutions by spent grain; *Proc. Biochem.* **36**(1) 59–64.
- Majumdar R K, Kar S, Talukdar D and Duttgupta T 2014 Geoelectric and geochemical studies for hydrological characterization of canning and adjoining areas of South 24 Parganas District, West Bengal; *J. Geol. Soc. India* **83** 21–30.
- Marinelli F and Niccoli W L 2000 Simple analytical equations for estimating ground water inflow to a mine; *Groundwater* **38**(2) 311–314.
- Mishra H K 1996 Comparative petrological analysis between the Permian coals of India and Western Australia: Paleoenvironments and thermal history; *Palaeogeogr. Palaeoclimatol. Palaeoecol.* **125** 199–216.
- Narany T S, Ramli M F, Fakharian K and Aris A Z 2016 A GIS-index integration approach to groundwater suitability zoning for irrigation purposes; *Arab. J. Geosci.*, <https://doi.org/10.1007/s12517-016-2520-9>.
- Pal P K, Paul S and Chatterjee R 2015 Estimation of *in-situ* stress and coal bed methane potential of coal seams from analysis of well logs, ground mapping and laboratory data in central part of Jharia Coalfield – An overview; In: *Petroleum Geosciences: Indian Contexts* (ed.) Soumyajit Mukherjee, Springer International Publishing, [https://doi.org/10.1007/978-3-319-03119-4\\_6](https://doi.org/10.1007/978-3-319-03119-4_6).
- Peksezer-Sayit A, Cankara-Kadioglu C and Yazicigil H 2014 Assessment of dewatering requirements and their anticipated effects on groundwater resources: A case study from the Caldag Nickel Mine, Western Turkey; *Mine Water Environ.*, <https://doi.org/10.1007/s10230-014-0306-4>.
- Plassard F, Winiarski T and Petit-Ramel M 2000 Retention and distribution of three heavy metals in a carbonated soil: Comparison between batch and unsaturated column studies; *J. Contam. Hydrol.* **42** 99–111.
- Rabeiy R E 2017 Assessment and modeling of groundwater quality using WQI and GIS in Upper Egypt area; *Environ. Sci. Pollut. Res.*, <https://doi.org/10.1007/s11356-017-8617-1>.
- Rajankar P N, Tambekar D H and Wate S R 2010 Groundwater quality and water quality index at Bhandara District; *Environ. Monit. Assess.* **179** 619–625, <https://doi.org/10.1007/s10661-010-1767-y>.
- Rajmohan N and Elango L 2004 Identification and evolution of hydro-geochemical processes in the groundwater environment in an area of the Palar and Cheyyar River Basins, southern India; *Environ. Geol.* **46** 47–61.
- Rapantova N, Grmela A, Vojtek D, Halir J and Michalek B 2007 Groundwater flow modeling applications in mining hydrogeology; *Mine Water Environ.* **26**(4) 264–270.
- Ravikumar P, Aneesul M M and Somashekar R K 2013 Water quality index to determine the surface water quality of Sankey tank and Mallathahalli lake, Bangalore urban district, Karnataka, India; *Appl. Water Sci.* **3** 247–261, <https://doi.org/10.1007/s13201-013-0077-2>.
- Rina K, Datta P S, Singh C K and Mukherjee S 2011 Characterization and evaluation of processes governing the groundwater quality in parts of the Sabarmati basin, Gujarat using hydrochemistry integrated with GIS; *Hydrol. Process.*, <https://doi.org/10.1002/hyp.8284>.
- Roy M D and Ghosh J K 2002 Final report on the regional exploration for coal in Krishnanagar Sector, Raniganj Coalfield, Bankura District, West Bengal; Coal Wing. Geological Survey of India; [http://www.portal.gsi.gov.in/gsiDoc/fspReports/CW/2000-2005/CW\\_CWPR02917\\_2000\\_2001\\_REPORT\\_1.pdf](http://www.portal.gsi.gov.in/gsiDoc/fspReports/CW/2000-2005/CW_CWPR02917_2000_2001_REPORT_1.pdf).
- Sadat-Noori S M, Ebrahimi K and Liaghat A M 2014 Groundwater quality assessment using the Water Quality Index and GIS in Saveh–Nobaran aquifer, Iran; *Environ. Earth Sci.* **71** 3827–3843, <https://doi.org/10.1007/s12665-013-2770-8>.
- Shah N, Nachabe M and Ross M 2007 Extinction depth and evapotranspiration from ground water under selected land covers; *Groundwater* **45** 329–338, <https://doi.org/10.1111/j.1745-6584.2007.00302.x>.
- Sahu P and Sikdar P K 2008 Hydrochemical framework of the aquifer in and around East Kolkata Wetlands, West



- Bengal, India; *Environ. Geol.* **55** 823–835, <https://doi.org/10.1007/s00254-007-1034-x>.
- Saaty T L 1980 *The analytic hierarchy process*; McGraw-Hill, New York.
- Shabbir R and Ahmad S S 2015 Use of Geographic information system and water quality index to assess groundwater quality in Rawalpindi and Islamabad; *Arab. J. Sci. Eng.*, <https://doi.org/10.1007/s13369-015-1697-7>.
- Simsek C and Gunduz O 2007 IWQ Index: A GIS-integrated technique to assess irrigation water quality; *Environ. Monit. Assess.* **128** 277–300, <https://doi.org/10.1007/s10661-006-9312-8>.
- Singh A K, Mahato M K, Neogi B, Mondal G C and Singh T B 2011 Hydrogeochemistry, elemental flux, and quality assessment of mine water in the Pootkee–Balihari mining area, Jharia coalfield, India; *Mine Water Environ.*, <https://doi.org/10.1007/s10230-011-0143-7>.
- Singh A K, Mondal G, Kumar S, Singh T, Tewary B and Sinha A 2008 Major ion chemistry, weathering processes and water quality assessment in upper catchment of Damodar River basin, India; *Environ. Geol.* **54** 745–758.
- Singh R N and Atkins A S 1985 Analytical techniques for the estimation of mine water inflow; *Int. J. Min. Eng.* **3** 65–77.
- Surinaidu L, Gurunadha Rao V V S, Srinivasa Rao N and Srinu S 2014 Hydrogeological and groundwater modeling studies estimate the groundwater inflows into the coal mines at different mine development stages using MODFLOW in Andhra Pradesh, India; *Water Resour. Industry*, <https://doi.org/10.1016/j.wri.2014.10.002>.
- Todd D K 1980 *Groundwater hydrology*; New York: Wiley, 535p.
- Todd D K and Mays L W 2005 *Groundwater hydrology*; 3rd edn, USA, 348p.
- Toran L and Grandstaff D 2002 PHREEQC and PHREEQCI: Geochemical modelling with an interactive interface; *Groundwater* **40(5)** 462–464.
- Trivedi P, Bajpai A and Thareja S 2009 Evaluation of water quality: Physico-chemical characteristics of Ganga River at Kanpur by using correlation study; *Nature Sci.* **1** 91–94.
- Unsal B and Yazicigi H 2015 Assessment of open pit dewatering requirements and pit lake formation for the Kışladağ Gold Mine, Uşak, Turkey; *Mine Water Environ.*, <https://doi.org/10.1007/s10230-015-0345-5>.
- Vasanthavigar M, Srinivasamoorthy K, Vijayaragavan K, Ganthi R R, Chidambaram S, Anandhan P, Manivannan R and Vasudevan S 2010 Application of water quality index for groundwater quality assessment: Thirumanimuttar sub-basin, Tamilnadu, India; *Environ. Monit. Assess.* **171** 595–609, <https://doi.org/10.1007/s10661-009-1302-1>.
- Vijaya, Tripathi A, Roy A and Mitra S 2012 Palynostratigraphy and age correlation of subsurface strata within the sub-basins in Singrauli Gondwana Basin, India; *J. Earth Syst. Sci.* **121(4)** 1071–1092.
- WHO 1997 *Guideline for drinking water quality: Recommendations*; 2nd edn, Vol. 1, Geneva: WHO.
- Wilson J D and Naff R L 2004 The U.S. Geological Survey Modular Ground-Water Model – GMG Linear Equation Solver Package Documentation; USGS Open-File Report 2004-1261.
- Zaidel J, Markham B and Bleiker D 2010 Simulating seepage into mine shafts and tunnels with MODFLOW; *Groundwater* **48(3)** 390–400.
- Zheng C and Bennett G D 2002 *Applied contaminant transport modelling*; 2nd edn, New York, pp. 296–301.

Corresponding editor: SUBIMAL GHOSH